



Synthesis and characterization for new Zn(II) complexes and their optimizing fertilization performance in planting corn hybrid

Ismail Althagafi¹ · Moataz Morad¹ · Aisha Y. Al-dawood¹ · Naema Yarkandy¹ · Hanadi A. Katouah¹ · Aisha S. Hossan⁴ · Abdalla M. Khedr^{1,5} · Nashwa M. El-Metwaly^{1,6} · Farag Ibraheem^{2,3}

Received: 25 July 2020 / Accepted: 19 November 2020 / Published online: 5 January 2021
© Institute of Chemistry, Slovak Academy of Sciences 2021, corrected Publication 2021

Abstract

Novel Zn(II)–benzohydrazide complexes have been synthesized using $Zn(NO_3)_2 \cdot 6H_2O$ salt. All new syntheses were investigated by available analytical and spectral tools to demonstrate their formulae. Binuclear complexes were proposed with all ligands through pentadentate mode of bonding. Octahedral geometry was the only structural form proposed for complexes. Benzohydrazide derivatives coordinate by the same mode, which point to negligible effect of *p*-substituents on donor site environment. This mode was verified basically by IR and ¹H, ¹³C NMR spectra. According to XRD patterns, crystallite particles of complexes were appeared in nanosized range. Such feature is preferable in variable application fields. Molecular modeling and molecular docking were interested in this study to strengthen experimental studies. One of these complexes [Zn(II)–H₂L²] was examined to be an additive optimizing the performance of traditional fertilizer (NH₄NO₃) in planting corn hybrid. This complex significantly improved components of photosynthetic carbon assimilation as photosynthetic pigments, sucrose, and soluble sugars. Interestingly, the applied complex induced responses, which were consistently higher than those treated by traditional fertilizer (NH₄NO₃). Therefore, these results highlight the promising behavior of Zn(II)–H₂L² complex in planting improvement.

Keywords Zn(II) complexes · DFT/B3LYP · Molecular docking · Fertilization optimizer · Photosynthesis

Supplementary Information The online version contains supplementary material available at <https://doi.org/10.1007/s11696-020-01440-7>.

✉ Nashwa M. El-Metwaly
n_elmetwaly00@yahoo.com

¹ Department of Chemistry, Faculty of Applied Science, Umm Al-Qura University, Makkah, Saudi Arabia

² Alqunfodah Research Unit, Umm Al-Qura University, Makkah, Saudi Arabia

³ Botany Department, Faculty of Science, Mansoura University, Mansoura 35516, Egypt

⁴ Chemistry Department, Faculty of Science, King Khalid University, P.O. Box 9004, Abha, Saudi Arabia

⁵ Chemistry Department, Faculty of Science, Tanta University, Tanta, Egypt

⁶ Chemistry Department, Faculty of Science, Mansoura University, Mansoura, Egypt

Introduction

A good attention is growing towards the synthesis of novel bio-active molecules using Zn(II) atom. This is due to their versatile geometries and coordination states that permit fine molecular engineering and physiological functions in living organisms. Such alongside with the modulation and/or improvement of ligand and photophysical characteristics by chelation, which reflects the influence of metal on organic ligands (Andelescu et al. 2018; Mendiguchia et al. 2015). Zn(II) complexes not only are facily available, but also they are generally less cytotoxic towards cells and are conveniently monitored (Hosseinpour et al. 2017). Hydrazide-type ligands possess a significant number of potential donor atoms; hence, they show versatility in metal chelation. Zn(II) and Cd(II) complexes that were prepared by green approach were exhibited anti-microbial, anti-tumor, and anti-oxidant activity (Alzahrani et al. 2020). The coordination mode depends on ligand type and nature of central atom. Benzohydrazide derivatives and their metal complexes introduced essential and interesting biological features, such

as anti-cancer, anti-oxidant, anti-bacterial, and anti-fungal (Paixão et al. 2017; Patil and Bendre 2018). Zn(II) and Sn(II) complexes were prepared by electrochemical process and displayed distinguish in silico results towards different tumor cells (Refat et al. 2020a, b). Green method was utilized to synthesize Fe (III), Cu (II), and Zn (II) complexes from Schiff's base derivative and Zn(II) complex displayed significant biological activity (Al-Hazmi et al. 2020). Furthermore, zinc is a significant element used by a small extent for crops, yet is essential to normal plant development and growth. Zinc plays several important roles in plants, including its major roles in photosynthesis, auxin activity, DNA transcription, and enzyme reactions (Kumar et al. 2017). Of all micronutrients, zinc is the one utmost predominating deficient in the production of corn, which is most likely to reduce a yield response when used as fertilizer. To overcome deficiencies, various zinc sources can be applied, involving zinc chelates and zinc sulfate. Continuing our research concerning designing novel bio-active molecules (Saad et al. 2017, 2018), this research idea was established based on new benzohydrazide derivatives, which we used previously in preparing Cu(II) complexes (Katouah et al. 2019). But herein, we have variable goals starting with their use to synthesize bi or poly-nuclear Zn(II) complexes. Then, all new synthesizes will be characterized by analytical, spectral, and conformational techniques. Second, and regarding the application part, we moved away from traditional application followed in previous related articles (Katouah et al. 2019). We selected Zn(II) complex to be examined as a composite fertilization-optimizer in planting corn hybrid plant. Such study will be conducted from a comparative view for differentiation. We already used $Zn(NO_3)_2$ salt to prepare these

complexes, which are enriched by two essential atoms for plants (N and Zn).

Experimental part

Reagents

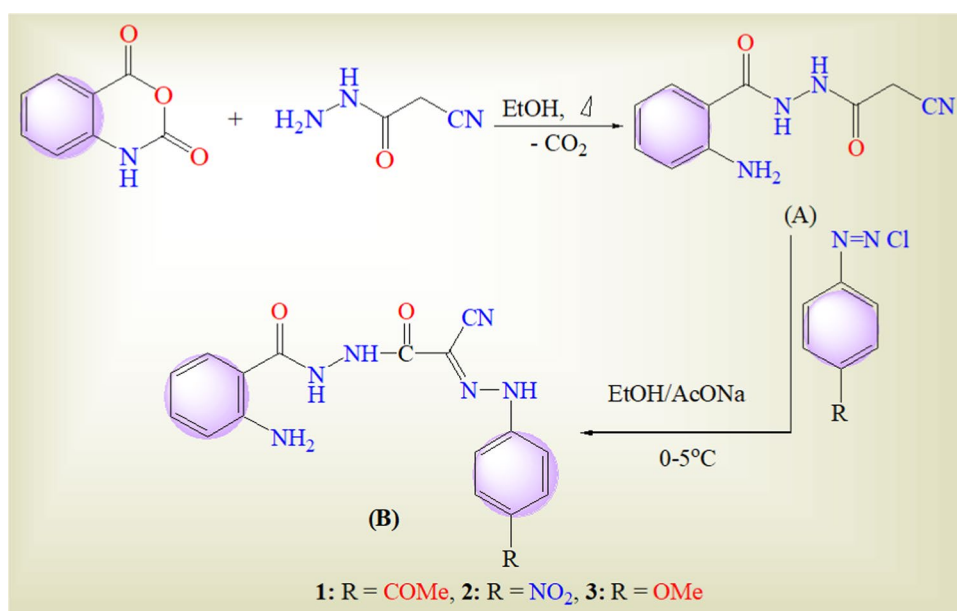
$Zn(NO_3)_2 \cdot 6H_2O$, isatoic anhydride, cyanoacetic hydrazide, *p*-anisidine, $NaNO_2$, HCl, ethanol, and DMSO were purchased from Sigma-Aldrich and utilized without any previous treatment.

Synthesis methodology

Synthesis of: 2-amino-N'-(2-cyanoacetyl)benzohydrazide (A)

Based on our previous preparation for these derivatives in which 0.05 mol (6.81 g) of isatoic anhydride suspended in ethanol (50 ml) were added to cyanoacetic hydrazide (0.05 mol, 4.95 g); the mixture was refluxed for 4 h; after cooling, the precipitate was formed. Desired off-white crystals for product A (Scheme 1) were filtered off and washed by ethanol. The yield was 67% and the m. p. is 173–175 °C. Moreover, the spectral bands for significant groups were; IR ($\bar{\nu}/cm^{-1}$): 3363, 3250 (NH_2 and NH), 2261 ($C\equiv N$), 1687, 1654 ($C=O$); and 1H NMR (Fig. 1S) ($DMSO-d_6$) peaks at; δ/ppm = 3.78 (s, 2H, CH_2), 6.40 (s, 2H, NH_2), 6.50 (t, 1H, Ar-H), 6.74 (d, 1H, Ar-H), 7.21 (t, 1H, Ar-H), 7.53 (d, 1H, Ar-H), 10.16 (s, 2H, 2NH) (Katouah et al. 2019).

Scheme 1 The synthesis process of benzohydrazide ligands (B; H_2L^{1-3})



Synthesis of: 2-amino-N'-(2-cyano-2-(arylhydrazono) acetyl)-benzohydrazide derivatives (B; H₂L¹-H₂L³)

According to our previous preparation (Katouah et al. 2019), in which 0.005 mol of NaNO₂ (0.345 g in 5 ml H₂O) was added slowly to 0.005 mol aniline derivatives suspension (p-nitroaniline, p-acetylaniline, or p-anisidine), which cold at 0–5°C in 1.5 ml HCl (conc.). Each diazonium chloride solution (freshly prepared) was added slowly to cold solution of compound A, (0.005 mol, 1.081 g) in ethanol/ sodium acetate (15 ml/3 g). The mixture of each reaction was stirred for 2 h at 0–5°C till precipitation. The products (Scheme. 1) were filtered off, washed, and recrystallized from ethyl alcohol to produce the derivatives (H₂L^{1–3}). All derivatives were characterized and reported (Katouah et al. 2019), 2-Amino-N'-(2-cyano-2-(4-acetylphenylhydrazono)acetyl) benzohydrazide (H₂L¹) is red powder derivative, and has yield of = 74%, m.p. = 205–207 °C. Its ¹H NMR (DMSO-*d*₆) spectrum showed; /ppm = 3.81 (s, 3H, OCH₃), 6.72 (s, 2H, NH₂), 6.90–7.85 (m, 8H, Ar–H), 10.22 (s, 1H, NH), 10.85 (s, 1H, NH), 11.15 (s, 1H, NH). 2-Amino-N'-(2-cyano-2-(4-nitrophenylhydrazono)acetyl) benzohydrazide(H₂L²) is a derivative, by yield = 68% and m.p. = 205–207 °C. 2-Amino-N'-(2-cyano-2-(4-anisylhydrazone) acetyl) benzohydrazide (H₂L³) is a reddish-brown derivative, by yield of = 57% and m.p. = 205–207 °C (Katouah et al. 2019). High similarity in spectral features of divers' derivatives may refer to the far-way position of substituents, which leads to non-remarkable effect on functional groups.

Synthesis of Zn(II)–HL^{1–3} complexes

5 mmol of Zn(NO₃)₂·6H₂O were dissolved in absolute ethanol and then added to ethanolic solution of ligand (2.5 mmol) as 2 M:1L molar ratio. Each reaction mixture was heated under reflux for 4–8 h, which varied from complex to another. The precipitates were filtered off, washed, and dried over anhydrous CaCl₂.

Application of proposed fertilizer

First, the corn hybrid plant has been cultivated in three boxes that irrigated by water for a few days. Then, one from boxes was irrigated by a suspension from Zn(II)–H₂L² complex (0.5 mmol, 0.409 g) and ammonia by 0.5 mmol (0.400 g). The second box was irrigated by free ammonia (NH₄NO₃, 1 mmol), while the third by water only.

Estimation of photosynthetic pigments

Using an ice-cold porcelain mortar, the photosynthetic pigments in a known weight of fresh leaves were grinded and

extracted in 80% acetone. The homogenates were transferred quantitatively to centrifuge tube, and centrifuged at 1000 rpm for 3 min. The remaining was washed many times by acetone, filtered off, and then, the filtrate was completed to definite volume (8 ml). The absorbance of clear extracts was recorded at 480, 644, and 663 nm, and the concentrations of photosynthetic pigments (chlorophyll a, chlorophyll b, and carotenoids) were calculated (ug/ml) as described previously (Metzner et al. 1965).

Estimation of sucrose and total sugar (TSS)

Using powdered dry leaves, the extraction of sugar was carried out. Known weights of powdered leaves (0.1 g), were mixed with alcohol and then shacked over-night. Each mixture was filtered off and washed, and then, the filtrates were completed (by alcohol) to known volume (10 ml) and kept in refrigerator. The sucrose was evaluated by 5.4 N KOH (0.1 ml), and 0.1 ml from extracts was hydrolyzed at 97 °C for 10 min. 3 ml fresh anthrone (150 mg in 100 ml H₂SO₄, 72%) were added to extracts. The mixtures were heated at 97 °C for 5 min. After cooling, the intensity of developed green color was spectrophotometrically determined at 620 nm (Handel 1968). The amount of sucrose was estimated using standard curve prepared by pure sugar. The sucrose concentrations were expressed as mg/g dry weight. TSS was evaluated in alcoholic extracts by mixing 0.1 ml with 3 ml fresh anthrone solution. The mixture was boiled in water both for 10 min and then cooled. The intensity was determined based on absorption at 625 nm. The amounts of TSS were evaluated using standard curve prepared using pure glucose (Yemm and Willis 1954). The data were statistically analyzed using COHORT/COSTAT program (798 Lighthouse Ave. PMB 329, Monterey, CA, 93,940, USA). The least significant difference (LSD) test was used to compare means with significance level at P ≤ 0.05.

Measurements techniques

Elemental content was determined using Perkin-Elmer 2400 CHN Elemental Analyzer, while zinc content was evaluated by complexometric titration (Vogel 1986). Molar conductivity of complexes was recorded upon JENWAY model 4070 conductance bridge. IR spectra for solid KBr disc and ¹H, ¹³CNMR (DMSO-*d*₆) were recorded on JASCO FT-IR-4100 spectrophotometer (400–4000 cm⁻¹) and Burker 500 MHz, respectively. Electronic spectra were conducted on UV₂ Unicam UV/Vis spectrophotometer in DMSO solvent. XRD patterns were obtained (10° < 2θ < 90° range) using X-ray diffractometer (GNR, APD2000PRO, Italy) with graphite mono-chromator (0.03° min⁻¹, Cu/Kα1 radiation). SEM

images were extracted using Joel JSM-6390 equipment. TGA and DTA analysis were executed on Shimadzu Thermogravimetric Analyzer (20–900 °C) by 10 °C min⁻¹ heating rate under nitrogen. Molecular modeling and molecular docking were conducted using known software (Gaussian09 or MOE-software).

Theoretical techniques

Molecular modeling

All syntheses were computationally treated to optimize their structural forms in ethanol solvent. Gaussian09 software (Frisch et al. 2010) was the program used for this conformation by applying DFT/B3LYP method under 6-31G basis set. The obtained files (chk and log), were visualized over Gauss-program screen (Dennington et al. 2007). Essential indexes were calculated by standard equations based on E_{HOMO} and E_{LUMO} energy gaps (ΔE).

Molecular docking

Using MOE module (Vs. 2015), docking process was executed over selected ligand (H_2L^2) and its Zn(II) complex (potential fertilizer) against three protein receptors (Alkhatib et al. 2020). This simulation process regarding two selected compounds was carried out versus, ligo, lbpd, and 5gmc protein–PDB files, which attributed to, *B. subtilis*, *P. aeruginosa*, and DNA-Helix, respectively. The co-crystalline couples (compound and protein) will be docked after the configuration steps. Regarding the tested compounds (inhibitors) must oriented by removing water molecules and adding hydrogen atoms. After that, the atomic charges must be added, and then, the potential energy fixed and other important parameters were adapted by MMFF94x force field, and then saved as MDB format. Second, protein PDB format was also configured by, adding hydrogen atoms over selected receptors followed by site-finder for searching sites over protein helix, so that the two sides (ligand and complex) were ready for docking

simulation process (Al-Nami et al. 2020). The process was the mean value of 30 poses, till stabilized docking complexes produced. Also, scoring-energy values were the average of trials by applying London dG scoring function. The function was upgraded using two unrelated refinements by triangle Matcher methods. The interaction parameters and docking complexes were extracted and discussed. The grad of inhibition was asserted referring to ligand types, receptor backbones (amino acids), interaction type, bond lengths, and scoring energies. Also, the length attributing to hydrogen-receptor bond must be not exceed than 3.5 Å (El-Metwaly et al. 2019).

Results and discussion

Physical features

Significant physical and analytical characteristics for all syntheses are exhibited in Table 1. All complexes have the same formula except the number of crystal water molecules (from 0 to 2). 2:1 molar ratio (Zn:L) was the only ratio proposed for all complexes, although changing of *p*-substituents. This may refer to farthest effect of such substituents on electron density over coordinating groups. Impact of charge transfer strength was easily noticed on the color of complexes that appeared with deep color instead of default color for Zn(II) complexes (white). All complexes are non-hygroscopic, having high m.p (~ 300 °C), and completely soluble in DMSO & DMF solvents. The conductivity of all complexes was determined for 1 mmol (Λ_m) and appeared with high conducting feature (95.85–107.54 Ω^{-1} cm² mol⁻¹). The conductivity values correspond to two nitrate groups attached ionically with coordination sphere (Geary 1971).

Mechanism of synthesis for benzohydrazides

Synthesis of 2-amino-*N'*-(2-cyanoacetyl)benzohydrazide (A) compound represents nucleophilic attack of amino part

Table 1 Physical and analytical data for ligands (H_2L^{1-3}) and their Zn(II) complexes

Compounds (Empirical formula)	Color	Λ_m (Ω^{-1} cm ² mol ⁻¹)	Elemental analysis (%) calcd (found)			
			C	H	N	M
(1) $\text{H}_2\text{L}^1(\text{C}_{18}\text{H}_{16}\text{N}_6\text{O}_3)$ (364.36)	Red		59.34 (59.36)	4.43 (4.44)	23.07 (23.08)	–
(2) $[\text{Zn}_2(\text{NO}_3)_2(\text{H}_2\text{L}^1)(\text{H}_2\text{O})_3](\text{NO}_3)_2 \cdot 2\text{H}_2\text{O}$ (833.21)	Deep Red	95.85	25.95 (25.94)	3.15 (3.11)	16.81 (16.78)	15.69 (15.70)
(3) $\text{H}_2\text{L}^2(\text{C}_{16}\text{H}_{13}\text{N}_7\text{O}_4)$ (367.32)	Reddish brown		52.32 (52.34)	3.57 (3.55)	26.69 (26.68)	–
(4) $[\text{Zn}_2(\text{NO}_3)_2(\text{H}_2\text{L}^2)(\text{H}_2\text{O})_3](\text{NO}_3)_2 \cdot \text{H}_2\text{O}$ (818.16)	Deep Brown	99.72	23.49 (23.49)	2.59 (2.55)	18.83 (18.80)	15.98 (15.99)
(5) $\text{H}_2\text{L}^3(\text{C}_{17}\text{H}_{16}\text{N}_6\text{O}_3)$ (352.13)	Reddish brown		57.95 (57.93)	4.58 (4.57)	23.85 (23.86)	–
(6) $[\text{Zn}_2(\text{NO}_3)_2(\text{H}_2\text{L}^3)(\text{H}_2\text{O})_3](\text{NO}_3)_2$ (784.96)	Brown	102.61	26.01 (26.02)	2.82 (2.80)	17.84 (17.83)	16.66 (16.67)

in cyanoacetic hydrazide towards carbonyl group of iso-toic anhydride. This conducts to open the ring, and then, decarboxylation was occurred. This behavior was confirmed through IR bands and NMR signals. The activity feature of methylene group in 2-amino-benzohydrazide (A) was verified against electrophilic diazo-coupling reaction. Such reaction was conducted using several diazonium chlorides, which yielded from five p-substituted aniline. Synthesized derivatives were characterized by analytical and spectral data.

Bonding mode

IR comparative studies

A comparative view for spectra of ligands and complexes leads to establish the mode of bonding inside coordination sphere (Table 2). Generally, neutral penta-dentate mode with two central atoms was proposed for all complexes. The lower shifted appearance of $\nu_{as}(\text{NH}_2)$, $\nu_s(\text{NH}_2)$, δNH_2 , $\nu\text{C}=\text{O}$, $\nu\text{C}=\text{N}$, and $\nu(\text{N}-\text{N})$ vibrations suggests their binding toward two zinc atoms. Good distribution for the binding sites along molecules gave best chance for the contribution of most of them across binuclear atoms. Synthesis of binuclear complexes, which they preliminary verified by IR spectra after elemental analysis, is the first goal in this study. New bands appeared at ≈ 770 and 670 cm^{-1} assign for $\delta_r(\text{H}_2\text{O})$ and $\delta_w(\text{H}_2\text{O})$ (El-Metwaly et al. 2005), and vibrations belong to coordinating water molecules.

Bands appeared at ≈ 1498 and 1387 cm^{-1} are attributing to $\nu_{as}(\text{NO}_3)$ and $\nu_s(\text{NO}_3)$ vibrations in mono-dentate binding mode ($\Delta > 100\text{ cm}^{-1}$) (El-Metwaly 2007). Also, the appearance of another band at $\approx 1346\text{ cm}^{-1}$ confirms the presence of nitrate anion attached with coordination sphere. The conductivity feature confirms the presence of two ionizable nitrate molecules. Moreover, other new bands appeared at low-frequency region ($< 600\text{ cm}^{-1}$) are attributing to $(\text{M}-\text{O})$ and $(\text{M}-\text{N})$ vibrations (Abu-Melha and El-Metwally 2008).

^1H & ^{13}C NMR study

NMR spectra were recorded for Zn(II) complexes, but they were sparingly soluble in DMSO- d_6 , and the signals are not clear. Extracted spectral data are displayed in Table 3. ^1H NMR spectral data have been compared with that of free ligands (reported previously in experimental part) to assert on bonding mode. The downshifted appearance of N^1H and N^3H , confirms their participation in coordination. Therefore, the contribution of two adjacent atoms (N atoms) point to presence of two coordinated zinc atoms, which agrees with previous analyses. More or less unshifted appearance of third NH proton confirms its ruling out from coordination. Also, a noticeable downshift of NH_2 signal from 3.72 ppm, confirms its participation in bonding. Moreover, ^{13}C NMR spectra assert on the formula proposed without alteration for bonding type of corresponding carbon atoms. All spectra appear with high similarity due to steady binding mode inside them. Such feature was

Table 2 Significant IR spectral bands (cm^{-1}) in the ligands (H_2L^{1-3}) and their Zn(II) complexes

Compounds	νOH , $\nu_{as}\text{NH}_2$, $\nu_s\text{NH}_2$	$\nu\text{C}\equiv\text{N}$	δNH_2	$\nu\text{C}=\text{O}$	$\nu\text{C}=\text{N}$, δNH_w	$\nu(\text{N}-\text{N})$	$\delta_r(\text{H}_2\text{O})$, $\delta_w(\text{H}_2\text{O})$	$\nu\text{M}-\text{O}$	$\nu\text{M}-\text{N}$
1) H_2L^1, 3357, 3366	2208	1615	1679, 1648	1547, 1462	1100	–	–	–
2) $[\text{Zn}_2(\text{NO}_3)_2(\text{H}_2\text{L}^1)(\text{H}_2\text{O})_3](\text{NO}_3)_2 \cdot 2\text{H}_2\text{O}$	3400, 3328, 3343	2211	1601	1665	1568, 1453	1089	769, 674	583	510
3) H_2L^2, 3449, 3366	2208	1601	1665	1545, 1461	1105	–	–	–
4) $[\text{Zn}_2(\text{NO}_3)_2(\text{H}_2\text{L}^2)(\text{H}_2\text{O})_3](\text{NO}_3)_2 \cdot \text{H}_2\text{O}$	3510, 3438, 3350	2219	1588	1654	1550, 1451	1096	773, 678	581	494
5) H_2L^3, 3489, 3373	2210	1613	1675, 1674	1584, 1458	1106	–	–	–
6) $[\text{Zn}_2(\text{NO}_3)_2(\text{H}_2\text{L}^3)(\text{H}_2\text{O})_3](\text{NO}_3)_2$	3496, 3470, 3350	2219	1595	1669, 1654	1592, 1449	1094	775, 669	569	486

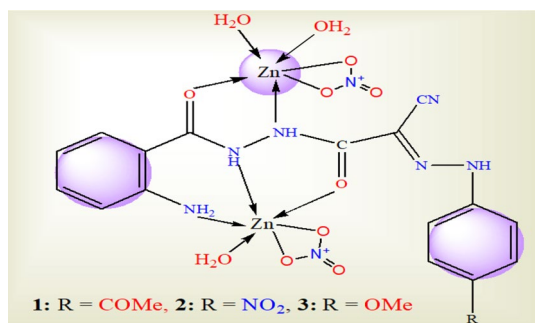
Table 3 DMSO- d_6 , ^1H & ^{13}C NMR data (ppm) for Zn(II) complexes

Compound	δ (s, NH_2)	δ (s, NNH)	δ (s, N^1HCO)	δ (s, CON^3H)	δ (CH_3-CO)	δ (C, Ar), (C, Ar)	(p-C, Ar)	δ (C=O)	δ (C=N)	δ (CN)
Zn(II) + H_2L^1	4.057	11.34	11.41	12.023	56.72, 39.20	129.23, 130.64	135.36	163.49	–	116.45
Zn(II) + H_2L^2	4.043	Broad at 9.75	–	–	–	115.24	130.62	215	160.50	117.23
Zn(II) + H_2L^3	–	–	–	–	46.41 (OCH ₃)	113.018	126.92	174.25	155.92	–

extracted from the expected appearance of carbon atoms without any abnormality.

Electronic transitions

UV–Vis spectra of all synthesized ligands (H_2L^{1-3}) were conducted in DMSO solvent. Also, their Zn(II) complexes were scanned over fixed range (200–700 nm). Although the absence of significant d–d transition bands, the observable shift for internal-ligand transitions beside charge transfer bands are not less important. A qualitative comparison for significant bands or shoulders is a judge for complexation process only. Transitions upon free C=O and C=N chromophoric groups (in free ligands) were appeared at; 35,520–36,567 and 29,451–32,671 cm^{-1} range, which assign for $\pi \rightarrow \pi^*$, transitions, respectively. Also, the appearance of shoulders at 37,542–38,952 cm^{-1} range is attributing to $n \rightarrow \sigma^*$ transition in NH groups. Narrow transition range for each group reflects more or less effect from *p*-substituents (explained previously). Whenever, the bands appeared $\approx 26,900$ cm^{-1} may assign for $n \rightarrow \pi^*$ transition. The interconnection of $n \rightarrow \pi^*$ bands with the visible region is referring to high conjugation presented inside the molecules which facilitate this transition type (Abou-Hussen et al. 2005). In complexes spectra, an observable blue shift was recorded over all transition types ($n \rightarrow \sigma^*$, $\pi \rightarrow \pi^*$ and $n \rightarrow \pi^*$) belong to coordinating groups (Lever 1986). Significant charge transfer shoulders were appeared near to $n \rightarrow \sigma^*$ transition, which affects significantly the color of Zn(II) octahedral complexes (Scheme 2).



Scheme. 2 The structural form of all binuclear Zn(II) complexes

XRD and SEM analysis

XRD is a fast technique mostly used upon homogenized solid compounds for identifying the phase of crystalline materials and can supply information on dimension for unit cell. A best knowledge about topographic structure, purity, and crystal lattice dynamics may be established (Cullity 1978). Diffraction patterns for all solid complexes (Fig. 3S) were obtained over a range of $10^\circ < 2\theta < 90^\circ$. All patterns differ significantly from the reactant materials which confirms the purity of these complexes. The comparison is based on referenced methods (Cullity 1993), upon the peak position and their relative intensities. The high degree of similarity between patterns confirms the extreme symmetry that cannot be ignored between resulting nano-crystals. This crystallinity feature may refer to regularity in coordination sphere around the same central atom though variable *p*-substituents. This reflects favorable impact of central atom on the orientation of active groups that readiness for complexation. Slow precipitation process leads to the best arrangement for crystal lattice. Crystallinity indexes were estimated based on full width at half maximum (FWHM). FWHM (β), relative intensity (%), 2θ , d-spacing, particle sizes, crystal strain (ϵ), and dislocation density (δ) are the significant indexes estimated using known equations (El-Sonbati et al. 2015; El-Metwaly et al. 2020; Velumani et al. 2003), (Table 4). All particle sizes (21.5–35.2 nm) obtained were appeared in nanometer range excellently; this feature reflects the promising application of such complexes. The distance between successive planes (hkl, d-spacing) computed for all crystals, appeared close to each other's (3.2455–3.2712 Å). This reflecting the high similarity between crystals prepared in their packing system. The crystal strain (ϵ) and dislocation density (δ) values were computed using; $\beta = \frac{\lambda}{S \cos \theta} - \epsilon \tan \theta$ and $\delta = 1/S^2$ equations, respectively. The two indexes are good indicators for crystal imperfections (dislocation of planes). Their reduced values reflect high uniformity and regularity of crystals under examination. SEM is the additive tool dealing with topographic property of solid surfaces. The surface images for investigated Zn(II) complexes (Fig. 4S) display two variable forms. Spherical form of the particles was observed for Zn(II)– H_2L^{1-3} complexes. The scale range applied for scanning technique reflects distinguish nanometer feature of all complexes in agreement with XRD results.

Table 4 XRD data over all Zn(II) nano-crystalline complexes

Compounds	Size (Å)	2θ	Intensity	d-spacing (Å)	ϵ	δ (Å ⁻²)	FWHM
[Zn ₂ (NO ₃) ₂ (H ₂ L ¹)(H ₂ O) ₃](NO ₃) ₂ ·2H ₂ O	3.5221	27.28	2124	3.2665	0.1113	0.0806	0.4231
[Zn ₂ (NO ₃) ₂ (H ₂ L ²)(H ₂ O) ₃](NO ₃) ₂ ·H ₂ O	2.2794	27.30	2540	3.2641	0.1718	0.1925	0.6538
[Zn ₂ (NO ₃) ₂ (H ₂ L ³)(H ₂ O) ₃](NO ₃) ₂	3.2297	27.38	2376	3.2548	0.1506	0.0959	0.4615

Moreover, the spherical shapes observed may point to the important influence of central atom on the particle accumulation process.

Thermal study

TGA analyses for the complexes were carried out at 20–900 °C rang and the plausible degradation has been displayed (Table 1S). This study emphasis the molecular formulae of complexes through plausible degradation schemes. TGA curves were appeared by two-to-three degradation stages. Three TGA curves started decomposition at low-temperature values (< 45 °C) except for Zn(II)–H₂L³ complex. This lower thermal stability was clearly combined with the presence of crystal water molecules. The thermal behavior of complexes is varied, which appeared in residual moieties that changed from one to another. While, other curves ended with high residual parts coincided with great masses from coordination environment. Such great masses may reflect the rigidity of coordinating bonds around central atom, as appeared in Zn(II)–H₂L^{1,3}. The high congruence between

practical mass loss and that calculated reflects acceptable degradation pathways suggested as well as precision for the boarder of each stage.

Theoretical studies

Molecular modeling in ethanol solution

This computation gives an extended view of the degree of activity of such compounds towards planned application. All Zn(II)–benzohydrazide complexes (H₂L^{1–3}) have been optimized (Fig. 1) by applying Gaussian09 program under DFT/B3LYP method in ethanol solution to simulate true behavior. Electrophilicity index (ω), electronegativity (χ), global hardness (η), chemical potential (μ), global softness (S), and absolute softness (σ) are the parameters computed based on frontier energy gaps (ΔE) (Table 2S) (El-Ayaan et al. 2007). Electrophilicity index (ω) is a best indicator for degree of acidic-reactivity or toxicity. Chemical potential (μ) and electronegativity (χ) are counter-parameters reflecting the ability of acquiring electrons from environment. Their values

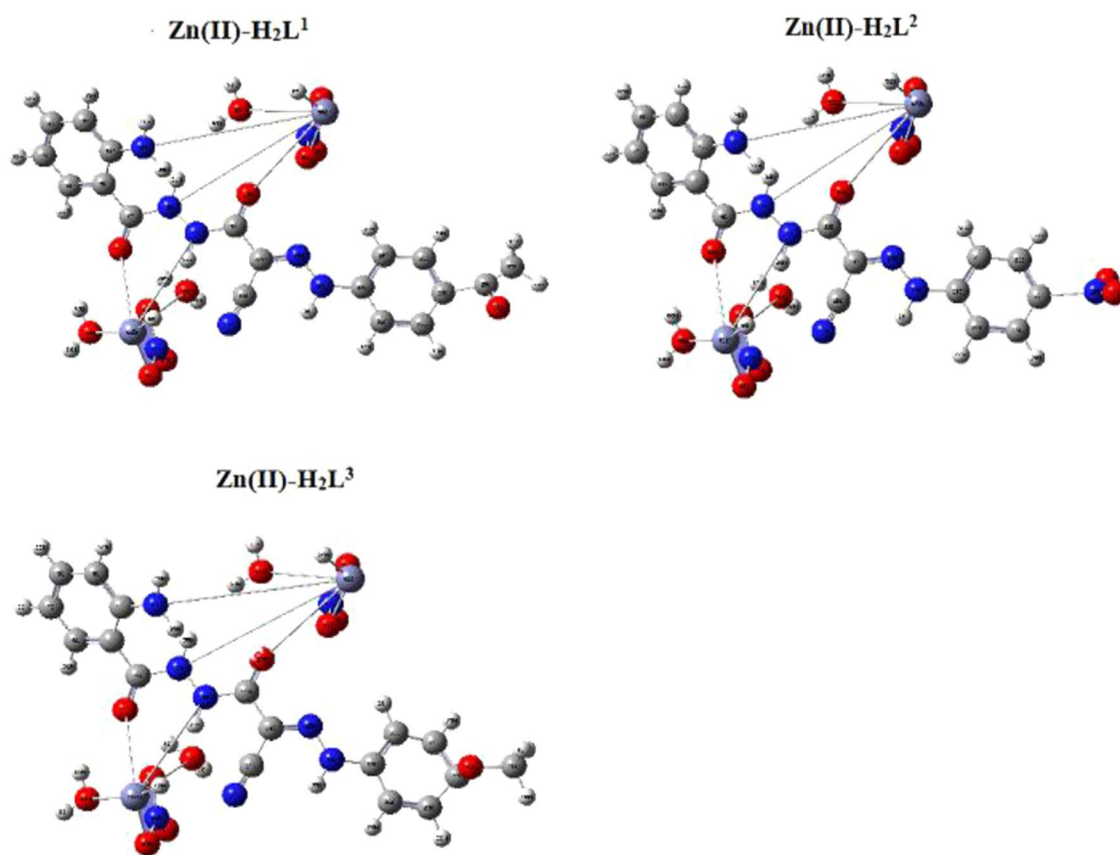


Fig. 1 The optimized structures for synthesized Zn(II) complexes

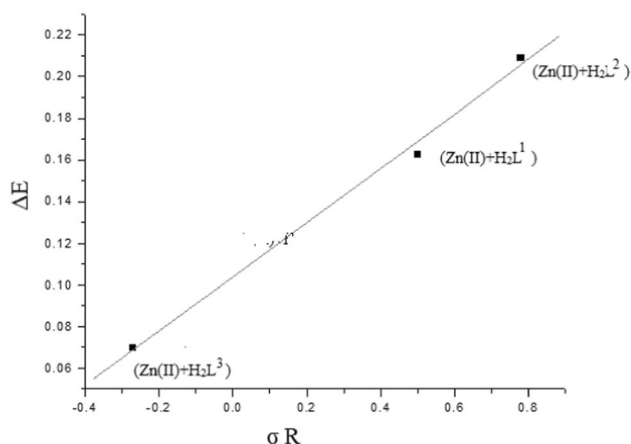


Fig. 2 Hammett's relation between (σR) and energy gaps (ΔE) for Zn(II) complexes

corresponding to Zn(II)-H₂L² complex display its advancement over the rest. Reduced ΔE values ($E_{\text{LUMO}} - E_{\text{HOMO}}$) which were observed clearly over all complexes reflect flexibility of inner electronic transitions. While, the high energy gap recorded for Zn(II)-H₂L² reflects its high stability which coherently attached with highly inductive *p*-substituent NO₂ group. Hammett's equation has been applied perfectly (Fig. 2) against ΔE which represent direct relation with σ values. Hardness and softness indexes exhibit relative hardness of Zn(II)-H₂L² complex among the others. Such complex was chosen for application process. The images of HOMO and LUMO levels for all complexes were extracted (Fig. 3). HOMO frontier level has appeared covered organic molecule in most complexes. However, Zn(II)-H₂L² complex, displayed its concentration over benzohydrazide moiety, while, Zn(II)-H₂L³ complex, displayed its concentration over 4-anisylhydrazono. Moreover, LUMO frontier level was mainly concentrated over cyanoacetyl moiety and *p*-substituted ring.

Significant computed parameters

Visualizing log files over program screen leads to extract significant parameters. Charges of coordinating atoms, formation energy, oscillator strength, excitation energy, and dipole moment (Table 3S) were obtained for complexes. The charges over atoms (O^{11,13}, N¹⁻³, and Zn^{39,45}) were significantly reduced in the complexes due to coordination (Raman et al. 2005). Also, the charges were very close because of high symmetry in correlation system which repeated in all complexes. Oscillator strength, which considered the indicator for elasticity in electronic transition inside the molecule,

fell within the normal range (0–1). The minimized value calculated for Zn(II)-H₂L² complex reflects their internal soft transition. Such proposal was confirmed by the value of excitation energy, which was minimized in two complexes in comparing to the others (Tripathi et al. 2013; Refat et al. 2020a, b). The calculated formation energies clarify the raised stability of Zn(II)-H₂L² complex among the rest, which agrees with previous data. The calculated dipole moments have been arranged as follows: Zn(II)-H₂L² > Zn(II)-H₂L¹ > Zn(II)-H₂L³ which coincide with the feature of *p*-substituents. The raised values may refer to highly inductive effect of their substituents that affect strongly on the polarity.

Molecular docking study

This study was used to give a good simulation inside infected cells after treatment with suggested inhibitors, to evaluate degree of inhibition. This study is a preliminary step before applying the complex as fertilization optimizer, to assert on its safety on Human health, rather may be benefit. Therefore, the impact of such complex on chosen pathogens will support the aim. MOE module (Vis 2015) was used to execute the docking of H₂L² derivative and its complex (fertilizer optimizer) towards Iigo, 1bpd, and 5gmc proteins. Such proteins attribute to, *B. subtilis*, *P. aeruginosa*, and DNA-Helix, respectively (Gross et al. 2015). Interaction parameters (Table 5) and docking patterns were obtained and displayed in Fig. 4. Concerning the docking feature of H₂L², the following remarks can be reported; (i) scoring-energy (S) values introduced the best docking complex of H₂L²-1bpd by -6.0478 (Kcal/mole). (ii) The ligational sites were N(3), O(11), and 6-ring. (iii) Amino acid receptors, which mainly interact, were Tyrosine, Glutamate, and Lysine. (iv) The binding types were appeared as, pi-H, pi-H, H-donor, and H-acceptor. Concerning the docking property of Zn(II)-H₂L² complex, the following remarks can be reported; (i) Scoring-energy(S) values introduced the high inhibitory effect for the tested complex against the three pathogens, especially of Zn(II)-H₂L²-1bpd complex by -10.0909(Kcal/mole). (ii) The ligational sites were N(1&3) and O(11&13). (iii) Amino acid receptors, which mainly interact, were Aspartate, Glutamate, and Arginine. (iv) The binding types were appeared only as H-donor and H-acceptor. Figure 4 displays the surface maps of docking complexes that built over line dummies without isolating receptor atoms. Most of the maps clarify the best occupation for two tested compounds inside protein grooves, which point to good interaction in between, except H₂L²-5gmc complex (Fadda et al. 2019). Finally, it is worthy to note that the promising impact of

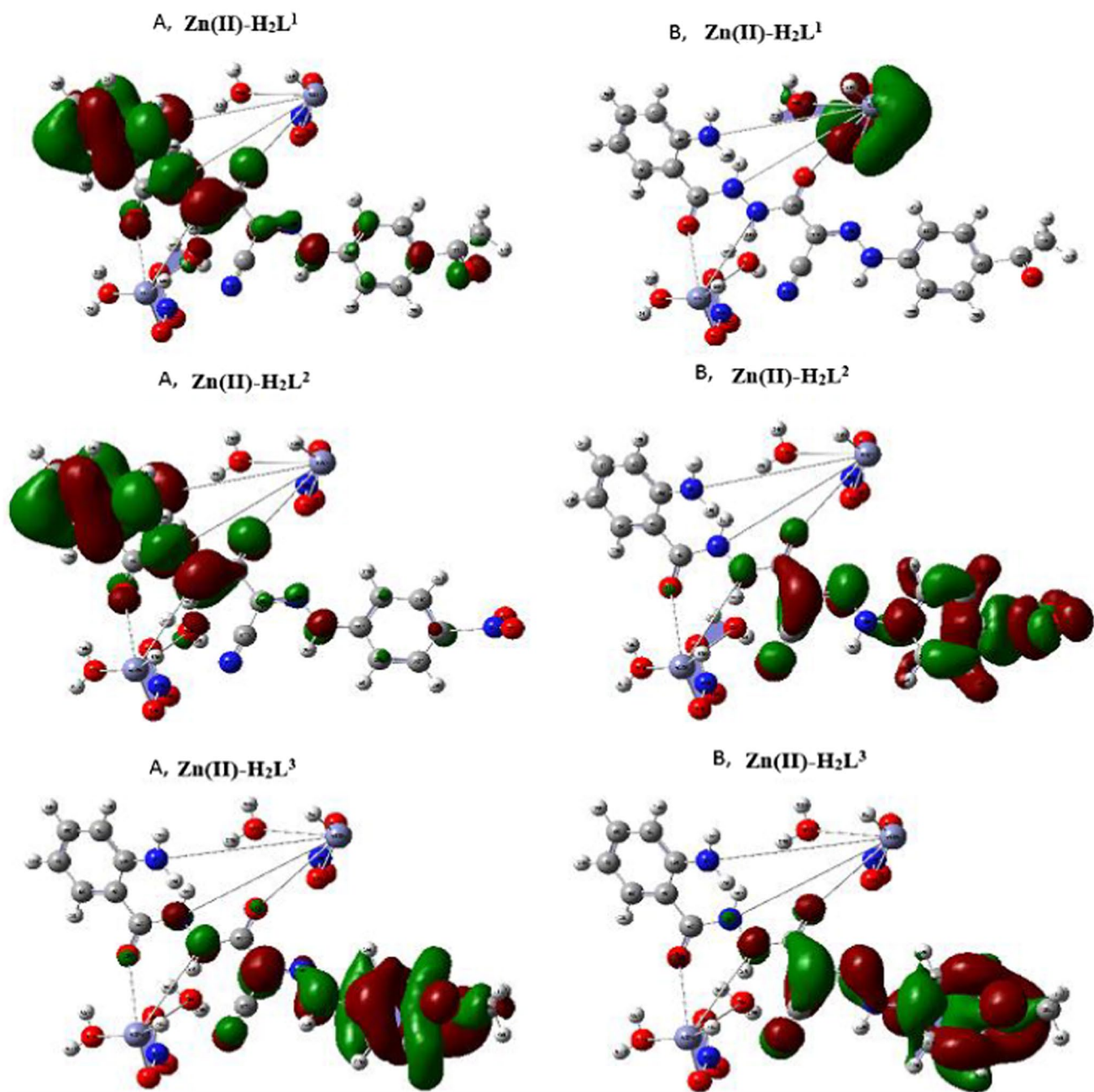


Fig. 3 Frontier molecular orbital images for treated Zn(II) complexes

fertilization optimizer not only as a plant-nutrient but also as pathogen inhibitor was clearly supported by this study.

Impact of Zn(II)–benzohydrazide application on physiology of corn hybrid plant

To test and evaluate the activity of $[\text{Zn}_2(\text{NO}_3)_2(\text{H}_2\text{L}^2)(\text{H}_2\text{O})_3](\text{NO}_3)_2 \cdot \text{H}_2\text{O}$ as fertilization optimizer in the presence of ammonia, it was applied to green-house grown plants.

Its impact on physiology of this plant was assessed. Our physiological analysis focused on leaves as they are the main organs in which critical physiological processes take place.

Changes in photosynthetic pigments

$\text{Zn}(\text{II})\text{-H}_2\text{L}^2$ - promotes changes in various photosynthetic pigments (a, b, Cars, and total pigments) in corn hybrid plant, were shown (Table 6). Compared to untreated

Table 5 Molecular docking data for potential fertilizer and free ligand against selected proteins

Compound	Protein	Ligand	Receptor	Interaction	Distance	E (Kcal/mol)	S (energy score)
H_2L^2	ligo	N 3	6-ring TYR 104 (A)	H-pi	3.44	– 1.4	– 5.8540
	1bpd	N 3	OE1 GLU 26 (A)	H-donor	3.33	– 1.9	– 6.0478
		O 11	NZ LYS 87 (A)	H-acceptor	2.97	– 2.3	
$Zn(II)-H_2L^2$	5gmc	6-ring	CA GLU 140 (A)	pi-H	3.26	– 0.9	– 5.2665
	ligo	N 1	O ILE 134 (B)	H-donor	3.22	– 1.4	– 6.4864
		O 13	OE2 GLU 18 (B)	H-donor	2.87	– 4.7	
	1bpd	O 11	OD1 ASP 276 (A)	H-donor	2.68	– 5.6	– 10.0909
		N 1	NH1 ARG 183 (A)	H-acceptor	3.16	– 1.9	
		N 3	NH2 ARG 183 (A)	H-acceptor	3.02	– 1.1	
	5gmc	N 1	NH2 GLU 140 (A)	H-acceptor	3.10	– 1.2	– 6.4214

plants, both traditional nitrogen fertilizer (NH_4NO_3) and mixed fertilizer ($Zn(II)-H_2L^2$ + ammonia) induced significant increases in all photosynthetic pigment fractions and total pigments. Mixed fertilizer increases photosynthetic pigments, which are always higher than those by NH_4NO_3 .

Changes in carbohydrate level

Table 6 shows $Zn(II)-H_2L^2$ -induced changes in sucrose and total soluble sugars. The tested complex as well as NH_4NO_3 encourage significant increases in both sucrose and TSS compared to other untreated plants. Mixed fertilizer (complex + ammonia) encourages increase in sugars concentrations, which noticeably higher than that of free NH_4NO_3 . Mixed fertilizer increases 1.32- and 2.77-fold in sucrose and total soluble sugars respectively (TSS). The results of our physiological analysis suggest successful absorption and use of $Zn(II)-H_2L^2$ in planting corn hybrid with exceeded features, and also increases photosynthetic pigments and sugars than that reported in many previous studies (Tóth et al. 2002; Ding et al. 2005). Therefore, the new complex directly provides nitrogen required to the synthesis of photosynthetic pigments and/or successfully interfered with their metabolic pathways. The complex improved photosynthetic pigments in leaves and their efficiency or capacity for light capture (Khamis et al. 1990). This may partially explain the high level of sucrose and total soluble sugars in leaves in response to complex applied in comparing to untreated or under NH_4NO_3 only (Kühn and Grof 2010).

It is worthy to note that new nitrogen and zinc-rich complex is considered fertilization optimizer for plant

growth and productivity. It is also contributes to protein and nucleic acid synthesis. In addition, Zn is important for biosynthesis of amino acid tryptophan, which is important for auxin phytohormone that controls cell division and plant growth (Hafeez et al. 2013).

Conclusion

This research was interested in new application approach dealing with economic progress. New $Zn(II)$ -benzohydrazide complexes were synthesized and fully characterized. Binuclear central atoms were proposed within octahedral configuration for all complexes. Also, all prepared complexes were fall in nanometer range by the excellent way. A chosen complex [$Zn(II)-H_2L^2$] really enriched with nutrients was used as fertilization optimizer in planting corn hybrid. Novel complex is rich in both N and Zn, which are important in the synthesis of various photosynthetic pigments as well as soluble sugars. Therefore, the new complex has a strong potential as multifunctional fertilizer, and also plays a considerable role as an inhibitor for three Human pathogens through molecular docking study. It would be interesting to investigate in detail the mode of action of this interesting complex and test its metabolic pathways in plants. Also, the inhibition effect of the new complex against two plant microbial diseases was considered a favorable additive for fertilizer, which may be used as a foliar fertilizer.

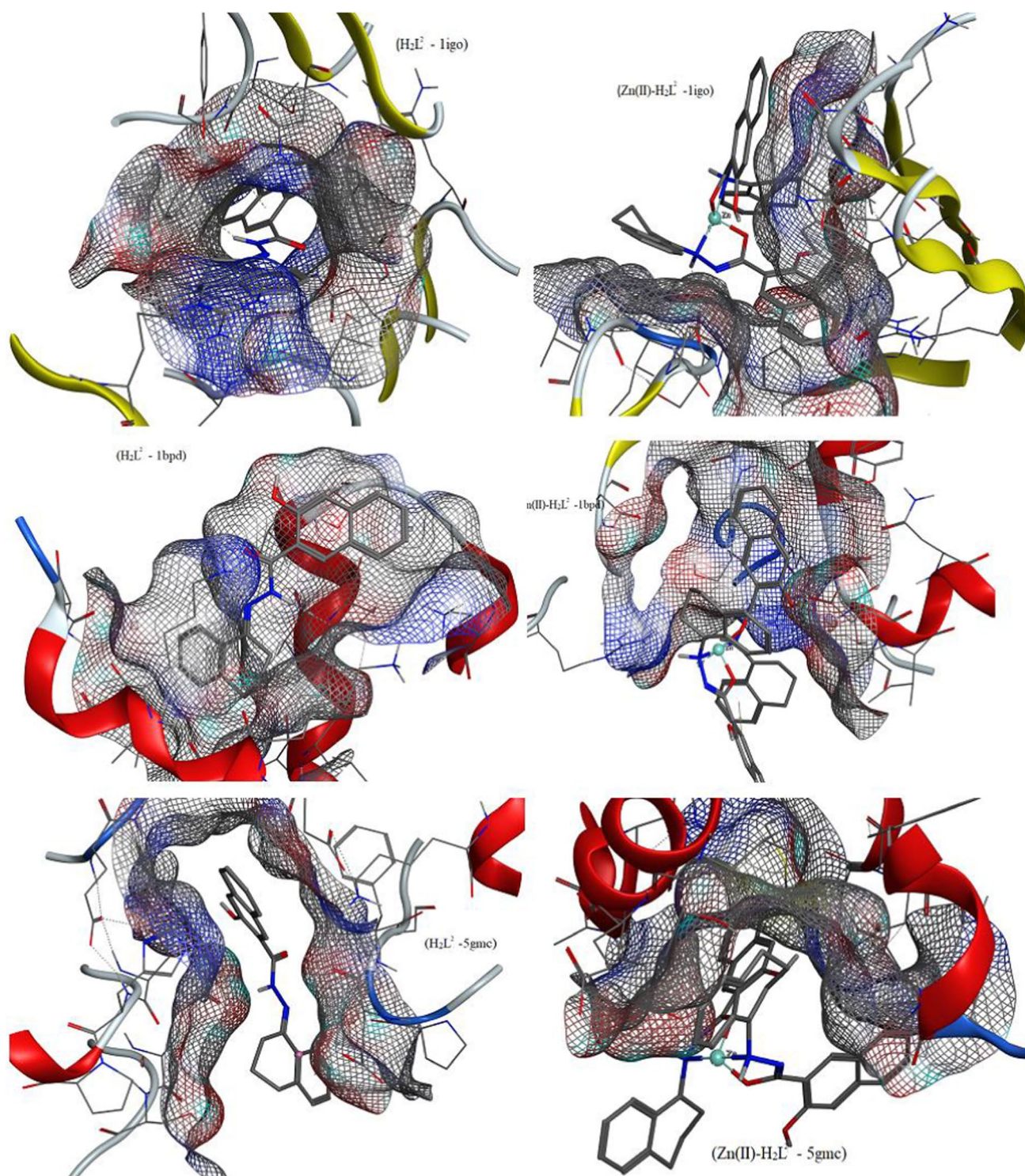


Fig. 4 Docking surfaces maps of alternative fertilizer complex [Zn(II)-H₂L²] and the free ligand (H₂L²) against selected proteins

Table 6 Comparative physiological responses of corn hybrid plants to different fertilizer treatments

Treatment	Photosynthetic pigments ($\mu\text{g/g F.WT}$)				Carbohydrates (mg/g Dwt)	
	Chlorophyll a	Chlorophyll b	Carotenoids	Total pigments	Sucrose	TSS
Zn(II)-H ₂ L ²	23.15 ^a	7.45 ^a	6.36 ^a	36.97 ^a	1.57 ^a	2.80 ^a
NH ₄ NO ₃	15.72 ^b	5.32 ^b	4.27 ^b	25.32 ^b	1.46 ^b	1.91 ^b
Non-fertilized	10.69 ^c	3.00 ^c	3.27 ^c	16.96 ^c	1.11 ^c	1.40 ^c

Shown values are the means of various fractions of photosynthetic pigments, sucrose, and total soluble sugars. Means with different letters indicate significant statistical difference among treatments at ($P \leq 0.05$)

Compliance with ethical standards

Conflict of interest The authors declare that there are no conflicts of interest.

References

- Abd El-Karim SS, Anwar MM, Mohamed NA, Nasr T, Elseginy SA (2015) Design, synthesis, biological evaluation and molecular docking studies of novel benzofuran-pyrazole derivatives as anticancer agents. *Bioorg Chem* 63:1–12. <https://doi.org/10.1016/j.bioorg.2015.08.006>
- Abou-Hussen AA, El-Metwaly NM, Saad EM, El-Asmy AA (2005) Spectral, magnetic, thermal and electrochemical studies on phthaloyl bis (thiosemicarbazide) complexes. *J Coord Chem* 58:1735–1749. <https://doi.org/10.1080/00958970500262270>
- Abu-Melha KS, El-Metwally NM (2008) Spectral and thermal studies for some transition metal complexes of bis(benzylthiocarbohydrazone) focusing on EPR study for Cu(II) and VO²⁺. *Spectrochim Acta A Mol Biomol Spectrosc* 70(2):277–283. <https://doi.org/10.1016/j.saa.2007.07.058>
- Al-Hazmi GAA, Abou-Melha KS, El-Metwaly NM, Althagafi I, Shaaban F, Zaky R (2020) Green synthesis approach for Fe (III), Cu (II), Zn (II) and Ni (II)-Schiff base complexes, spectral, conformational, MOE-docking and biological studies. *Appl Organomet Chem* 34(3):e5403. <https://doi.org/10.1002/aoc.5403>
- Alkhatib F, Hameed A, Sayqal A, Bayazeed AA, Alzahrani S, Al-Ahmed ZA, Zaky R, El-Metwaly NM (2020) Green-synthesis and characterization for new Schiff-base complexes; spectroscopy, conductometry, Hirshfeld properties and biological assay enhanced by in-silico study. *Arab J Chem* 13(8):6327–6340. <https://doi.org/10.1016/j.arabjc.2020.05.033>
- Al-Nami SY, Aljuhani E, Althagafi I, Abumelha HM, Bawazeer TM, Al-Solimiy AM, Al-Ahmed ZA, Al-Zahrani F, El-Metwaly N (2020) Synthesis and Characterization for new nanometer Cu(II) complexes, conformational study and molecular docking approach compatible with promising in vitro screening. *Arab J Sci Eng* 2020:1–18. <https://doi.org/10.1007/s13369-020-04814-x>
- Alzahrani S, Morad M, Bayazeed A, Aljohani MM, Alkhatib F, Shah R, Katouah H, Abumelha HM, Althagafi I, Zaky R, Metwaly NM (2020) Ball milling approach to prepare new Cd(II) and Zn(II) complexes; characterization, crystal packing, cyclic voltammetry and MOE-docking agrees with biological assay. *J Mol Struct* 1218:128473. <https://doi.org/10.1016/j.molstruc.2020.128473>
- Andelescua AA, Cretu C, Sasca V, Marinescu S, Cseh L, Costisor O, Szerb EI (2018) New heteroleptic Zn(II) and Cu(II) complexes with quercetine and N^N ligands. *Polyhedron* 147:120–125. <https://doi.org/10.1016/j.poly.2018.03.016>
- Cullity BD (1978) Elements of X-ray diffraction. Addison-Wesley Inc, Wembley
- Cullity BD (1993) Elements of X-ray diffraction. Addison-Wesley Inc., Boston
- Dennington R, Keith T, Millam J (2007) Gauss view, version 4.1.2. Semichem Inc., Shawnee Mission, Shawnee
- Ding L, Wang KJ, Jiang GM, Biswas DK, Xu H, Li LF, Li YH (2005) Effects of nitrogen deficiency on photosynthetic traits of maize hybrids released in different years. *Ann Bot* 96(5):925–930. <https://doi.org/10.1093/aob/mci244>
- El-Ayaan U, El-Metwally NM, Youssef MM, El Bialy SAA (2007) Perchlorate mixed-ligand copper(II) complexes of β -diketone and ethylene diamine derivatives: thermal, spectroscopic and biochemical studies. *Spectrochim Acta A Mol Biomol Spectrosc* 68(5):1278–1286. <https://doi.org/10.1016/j.saa.2007.02.011>
- El-Metwaly NM (2007) Spectral and biological investigation of 5-hydroxyl-3-oxopyrazoline 1-carbothiohydrazone and its transition metal complexes. *Transition Met Chem* 32:88–94. <https://doi.org/10.1007/s11243-006-0135-9>
- El-Metwaly NM, El-Shazly RM, Gabr IM, El-Asmy AA (2005) Physical and spectroscopic studies on novel vanadyl complexes of some substituted thiosemicarbazides. *Spectrochim Acta A Mol Biomol Spectrosc* 61(6):1113–1119. <https://doi.org/10.1016/j.saa.2004.06.027>
- El-Metwaly NM, Bondock S, Althagafi I, Khedr AM, Al-Zahar AA, Saad FA (2019) Investigating the influence of p-substituents upon spectral, thermal, kinetic, molecular modeling and molecular docking characteristics of new synthesized arylazobithiazolyl hydrazones. *Bull Chem Commun* 51(4):527–540. <https://doi.org/10.34049/bcc.51.4.5041>
- El-Metwaly N, Katouah H, Aljuhani E, Alharbi A, Alkhatib F, Aljohani M, Alzahrani S, Alfaifi MY, Khedr AM (2020) Synthesis and elucidation for new nanosized Cr(III)-pyrazolin complexes; crystal surface properties, antitumor simulation studies beside practical apoptotic path. *J Inorg Organomet Polym* 30:4142–4154. <https://doi.org/10.1007/s10904-020-01561-2>
- El-Sonbati AZ, Diab MA, El-Bindary AA, Mohamed GG, Morgan SM (2015) Thermal, spectroscopic studies and hydrogen bonding in supramolecular assembly of azo rhodanine complexes. *Inorg Chim Acta* 430:96–107. <https://doi.org/10.1016/j.ica.2015.02.031>
- Fadda AA, Abdel-Latif E, Fekri A, Mostafa AR (2019) Synthesis and docking studies of some 1,2,3-benzotriazine-4-one derivatives as potential anticancer agents. *J Heterocycl Chem* 56:804–814. <https://doi.org/10.1002/jhet.3452>
- Frisch MJ, Trucks GW, Schlegel HB (2010) Gaussian 09, Revision D. Gaussian Inc., Wallingford
- Geary WJ (1971) The use of conductivity measurements in organic solvents for the characterization of coordination compounds. *Coord Chem Rev* 7:81–122. [https://doi.org/10.1016/S0010-8545\(00\)80009-0](https://doi.org/10.1016/S0010-8545(00)80009-0)

- Gross S, Rahal R, Stransky N, Lengauer C, Hoefflich KP (2015) Targeting cancer with kinase inhibitors. *J Clin Invest* 125(5):1780–1789. <https://doi.org/10.1172/JCI76094>
- Hafeez B, Khanif YM, Samsuri AW, Radziah O, Zakaria W, Saleem (2013) Direct and residual effects of zinc on zinc-efficient and zinc-inefficient rice genotypes grown under low-zinc-content submerged acidic conditions. *Commun Soil Sci Plant Anal* 44(15):2233–2252. <https://doi.org/10.1080/00103624.2013.803558>
- Handel E (1968) Direct microdetermination of sucrose. *Anal Biochem* 22(2):280–283. [https://doi.org/10.1016/0003-2697\(68\)90317-5](https://doi.org/10.1016/0003-2697(68)90317-5)
- Hosseinpour S, Hosseini-Yazdi SA, White J (2017) Binuclear zinc(II) complexes of N(4)-substituted bis(thiosemicarbazone) ligands incorporating hydroxyl group and their non-hydroxyl analogues. *Inorg Chim Acta* 461:150–160. <https://doi.org/10.1016/j.ica.2017.02.022>
- Katouah HA, Al-Fahemi JH, Elghalban MG, Saad FA, Althagafi IA, El-Metwaly NM, Khedr AM (2019) Synthesis of new Cu(II)-benzohydrazide nanometer complexes, spectral, modeling, CT-DNA binding with potential anti-inflammatory and anti-allergic theoretical features. *Mater Sci Eng C* 96:740–756. <https://doi.org/10.1016/j.msec.2018.11.034>
- Khamis S, Lamaze T, Lemoine Y, Foyer C (1990) Adaptation of the photosynthetic apparatus in maize leaves as a result of nitrogen limitation - relationships between electron-transport and carbon assimilation. *Plant Physiol* 94:1436–1443. <https://doi.org/10.1104/pp.94.3.1436>
- Kühn C, Grof CP (2010) Sucrose transporters of higher plants. *Curr Opin Plant Biol* 13(3):287–297. <https://doi.org/10.1016/j.pbi.2010.02.001>
- Kumar M, Roy S, Faizi MSH, Kumar S, Singh MK, Kishor S, Peter SC, John RP (2017) Synthesis, crystal structure and luminescence properties of acenaphthene benzohydrazide based ligand and its zinc(II) complex. *J Mol Struct* 1128:195–204. <https://doi.org/10.1016/j.molstruc.2016.08.004>
- Lever API (1986) *Inorganic electronic spectroscopy*. Elsevier, Amsterdam
- Mendiguchia BS, Aiello I, Crispini A (2015) Zn(II) and Cu(II) complexes containing bio-active O, O-chelated ligands: homoleptic and heteroleptic metal-based biomolecules. *Dalton Trans* 44:9321–9334. <https://doi.org/10.1039/C5DT00817D>
- Metzner H, Rau H, Senger H (1965) Untersuchungen zur Synchronisierbarkeit einzelner Pigmentmangel-Mutanten von *Chlorella*. *Planta* 65:186–194. <https://doi.org/10.1007/BF00384998>
- Paixão DA, Marzano IM, Jaimes EHL, Pivatto M, Campos DL, Pavan FR, Deflon VM, Maia PS, Ferreira AMDC, Uehara IA, Silva MJB, Botelho FV, Pereira-Maia EC, Guillard S, Guerra W (2017) Novel copper(II) complexes with hydrazides and heterocyclic bases: Synthesis, structure and biological studies. *J Inorg Biochem* 172:138–146. <https://doi.org/10.1016/j.jinorgbio.2017.04.024>
- Patil M, Bendre R (2018) Synthesis, characterization and antioxidant potency of naturally occurring phenolic monoterpenoids based hydrazide motifs. *Med Chem (Los Angel)* 8:177–183. <https://doi.org/10.4172/2161-0444.1000509>
- Raman N, Johnsonraja TC (2005) Synthesis, spectral characterization, redox and antimicrobial activity of Schiff base transition metal(II) complexes derived from 4-aminoantipyrine and 3-salicylideneacetylacetone. *Cent Eur J Chem* 3:537–555. <https://doi.org/10.2478/BF02479281>
- Refat M, El-Metwaly NM, Sayqal A, Althagafi I, Abumelha HM, Katouah H, Al-Solimy AM, Shah R, Amin RR, Yamany YB, Al-Humaidi JY (2020a) Elaborated computational studies for Zn(II) and Sn(II) complexes, electro-synthesis, spectral, thermal and electrochemical analysis. *J Mol Liq* 309:113119. <https://doi.org/10.1016/j.molliq.2020.113119>
- Refat M, El-Metwaly NM, Yamany YB, Althagafi I, Hameed A, Alharbi A, Abualnaja M, Shah R, Al-Brakati A, Al-Humaidi JY (2020b) Electrochemical synthesis for new thiosemicarbazide complexes, spectroscopy, cyclic voltammetry, structural properties, and in silico study. *Appl Organomet Chem Early View*. <https://doi.org/10.1002/aoc.6049>
- Saad FA, Elghalban MG, El-Metwaly N, El-Ghamry H, Khedr AM (2017) Density functional theory/B3LYP study of nanometric 4-(2,4-dihydroxy-5-formylphen-1-ylazo)-N-(4-methylpyrimidin-2-yl)benzenesulfonamide complexes: Quantitative structure–activity relationship, docking, spectral and biological investigations. *Appl Organomet Chem* 31(10):e3721. <https://doi.org/10.1002/aoc.3721>
- Saad FA, Al-Fahemi JH, El-Ghamry H, Khedr AM, Elghalban MG, El-Metwaly NM (2018) Elaborated spectral, modeling, QSAR, docking, thermal, antimicrobial and anticancer activity studies for new nanosized metal ion complexes derived from sulfamerazine azodye. *J Therm Anal Calorim* 131(2):1249–1267. <https://doi.org/10.1007/s10973-017-6598-4>
- Tóth R, Mészáros I, Veres S, Nagy J (2002) Effects of the available nitrogen on the photosynthetic activity and xanthophyll cycle pool of maize in field. *J Plant Physiol* 159(6):627–634. <https://doi.org/10.1078/0176-1617-0640>
- Tripathi SK, Muttineni R, Singh SK (2013) Extra precision docking, free energy calculation and molecular dynamics simulation studies of CDK2 inhibitors. *J Theor Biol* 334:87–100. <https://doi.org/10.1016/j.jtbi.2013.05.014>
- Velumani S, Mathew X, Sebastian PJ, Narayandass SK, Mangalaraj D (2003) Structural and optical properties of hot wall deposited CdSe thin films. *Sol Energy Mater Sol Cells* 76:347–358. [https://doi.org/10.1016/S0927-0248\(02\)00287-8](https://doi.org/10.1016/S0927-0248(02)00287-8)
- Vogel AI (1986) *Text book of quantitative inorganic analysis*. Longman, London
- Yemm EW, Willis AJ (1954) The estimation of carbohydrates in plant extracts by anthrone. *Biochem J* 57(3):508–514. <https://doi.org/10.1042/bj0570508>

Publisher's Note Springer Nature remains neutral with regard to jurisdictional claims in published maps and institutional affiliations.